



Contents lists available at ScienceDirect

Journal of Monetary Economics

journal homepage: www.elsevier.com/locate/jmonecoUnemployment crises[☆]Nicolas Petrosky-Nadeau^a, Lu Zhang^{b,c,*}^a Federal Reserve Bank of San Francisco, 101 Market Street, San Francisco CA 94105, USA^b Fisher College of Business, The Ohio State University, 760A Fisher Hall, 2100 Neil Avenue, Columbus OH 43210, USA^c NBER, USA

ARTICLE INFO

Article history:

Received 8 April 2019

Revised 22 January 2020

Accepted 27 January 2020

Available online xxx

JEL classification:

E24

E32

J63

J64

Keywords:

Search model of equilibrium unemployment

The great depression

The unemployment volatility

Economic history

Globally nonlinear solution

ABSTRACT

An equilibrium search model with credible bargaining, when calibrated to the mean and volatility of postwar unemployment rates, is a good start to understanding the unemployment crisis in the Great Depression. Drawing from rarely used data sources, this paper compiles historical monthly time series of U.S. unemployment rates, vacancy rates, and labor productivity, some of which date back to 1890. The frequency, persistence, and severity of the unemployment crises in the model are quantitatively consistent with those in the historical data.

Published by Elsevier B.V.

1. Introduction

The macro labor literature has traditionally focused on the second moments of the labor market in the postwar sample. As a fundamental departure, this paper asks to what extent the search model of equilibrium unemployment can quantitatively explain the long-run historical facts of U.S. labor market, including the Great Depression in the 1930s. Drawing from a

[☆] For helpful comments, we thank Hang Bai, Andrew Chen, Daniele Coen-Pirani, Steven Davis, Mariacristina De Nardi, Paul Evans, Wouter Den Haan, Bob Hall, Rafael Lopez de Melo, Dale Mortensen, Morten Ravn, Paulina Restrepo-Echavarría, Robert Shimer, Etienne Wasmer, Randall Wright, Francesco Zanetti, and seminar participants at Federal Reserve Bank of San Francisco, Northwestern University, The Ohio State University, University of Georgia, University of California at Irvine, University of California at Los Angeles, Université du Québec à Montréal, University of California at Berkeley, University of California at Santa Cruz, University of Southern California, Kiel Institute, Sciences Po Paris, University College London, University of Montreal, University of Texas at Austin, and University of Edinburgh, as well as 19th International Conference on Computing in Economics and Finance at Society for Computational Economics, 2013 North American Summer Meeting of the Econometric Society, Southwest Search and Matching workshop at University of Colorado at Boulder, 2014 meeting of the Canadian Economic Association, Oslo New Developments in Business Cycle Analysis conference, 2014 NBER Summer Institute Macro Perspectives Workshop, and Deutsche Bundesbank Spring 2019 Conference on "Systematic Risk and the Macroeconomy." Rui Gong and Patrick Kiernan provided exemplary research assistance. Urban Jermann (the Editor) and an anonymous referee deserve special thanks. Nicolas Petrosky-Nadeau thanks Stanford Institute for Economic Policy Research and the Hoover Institution at Stanford University for their hospitality. The views expressed are those of the authors and do not necessarily reflect the position of the Federal Reserve Bank of San Francisco or the Federal Reserve System.

* Corresponding author.

E-mail addresses: Nicolas.Petrosky-Nadeau@sf.frb.org (N. Petrosky-Nadeau), zhanglu@fisher.osu.edu (L. Zhang).

variety of rarely used data sources, our first contribution is to compile the historical monthly series of unemployment rates and labor productivity dated back to January 1890 as well as vacancy rates dated back to January 1919. Our historical series reveal intriguing stylized facts, some of which have received little attention in the prior literature.

It is well known that the unemployment rates are extraordinarily high in the prewar sample, especially in the Great Depression. From 1931 to 1939, the average civilian unemployment rate is 14.8%, and the highest hits 25.5% in July 1932. In contrast, from 1951 to 2017, the mean unemployment rate is only 5.8%, and the maximum never exceeds 11%. We fit a three-state Markov chain on the historical series via maximum likelihood. Identifying months in which unemployment rates are above 15% as the crisis state, we estimate the unconditional probability of an unemployment crisis to be 2.93% and its persistence (the probability of a crisis next period conditional on a crisis in the current period) to be 91.11% in the 1890–2017 sample. Finally, the quarterly volatility of the unemployment rates is 25.8% in the 1890–2017 sample, more than doubling that of 12.6% in the post-1951 sample.

In contrast, the nonlinear dynamics in the vacancy rates are more muted. The quarterly volatility of the vacancy rates is 17.2% in the 1919–2017 sample and is only slightly higher than 13.5% in the post-1951 sample. However, the quarterly volatility of the vacancy-unemployment ratio (labor market tightness) is 37.9% in the historical sample, in contrast to only 25.6% in the postwar sample. The U.S. Beveridge curve is flatter in the historical sample than that in the postwar sample, as the unemployment-vacancy correlations are -0.79 and -0.92 across the two samples, respectively. Finally, the labor productivity is substantially more volatile in the historical sample than that in the postwar sample, 3.9% versus 1.2% per quarter. However, the early sample likely contains a fair amount of measurement errors.

Our second contribution is to quantify the extent to which the search model of equilibrium unemployment can explain the stylized facts in the U.S. labor market. We adopt the [Hall and Milgrom \(2008\)](#) framework because its equilibrium wage is derived from a credible bargaining game, which seems more realistic than the standard Nash bargaining game in describing the wage determination in the Great Depression. Relative to the Nash wage, the Hall-Milgrom wage is more insulated from the aggregate conditions in the labor market.

Our key insight is that the search model is a good start to explaining the large labor market dynamics in the historical sample. When calibrated to the mean of 5.8% and the volatility of 12.6% of the postwar unemployment rates, the model implies the persistence of the crisis state to be 91.8% and its unconditional probability 4.77%, which are close to 91.11% and 2.93% in the historical sample, respectively. The model also succeeds in generating a flatter Beveridge curve in crises than in normal periods. However, the model predicts an unemployment volatility of 15.6% in crises, falling short of 25.8% in the historical data. The model also predicts a market tightness volatility of 30.3% in crises, falling short of 37.9% in the data.

Credible bargaining plays a key role. From comparative statics, the probability of bargaining breakdown and the firm's delaying costs during each round of alternating offers are quantitatively important for explaining the unemployment crises. A higher probability of breakdown, in which both parties take outside options, brings credible bargaining closer to the Nash bargaining and makes wages more responsive to labor market conditions. As such, the crisis dynamics are dampened. In contrast, higher delaying costs make wages more insulated from labor market conditions and strengthen the crisis dynamics.

We feed the measured labor productivity in the Great Depression into the model, compute its implied sample paths, and compare them with those observed in the 1930s. The model does a good job in accounting for the large output decline and high unemployment rates in the Great Depression. Our measured log labor productivity indicates a large negative shock in 1933 with a magnitude of 3.4 unconditional standard deviations of that in the postwar sample. With the 1929 level scaled to 100, real output per capita in the data falls to 73.7 in 1933, recovers to 94.9 in 1936, but declines back to 81.1 in 1939. The model predicts a steeper drop to 64.2 in 1933, a slightly stronger recovery to 98.3 in 1936, and a lower level of 76.4 in 1939. In the data, civilian unemployment rates reach the highest level of 23.5%, and private nonfarm unemployment rates, 33.4%, in March 1933. The model predicts high unemployment rates above 32% from March to August, with the highest, 32.9%, in June, of 1933. Afterward, unemployment rates fall in the model to the 5.6%–8.8% range in 1936, which is lower than the 9.2%–11% range for civilian unemployment rates in the data. After 1936, unemployment rates are persistently high both in the model and in the data.

We also demonstrate the impact of detrending on accounting for the Great Depression. Our quantitative results, which are based on an annual smoothing parameter of 25 in the [Hodrick and Prescott \(1997\)](#) filter, are robust to a large range of alternative parameter values. The lower value of 6.25, which corresponds to 1600 in quarterly data, measures shorter cyclical fluctuations in the postwar data and treats the large movements in the Great Depression as changes in the trend itself. With 6.25, the measured log productivity experiences a negative shock with a magnitude of only 2.1 unconditional standard deviations in 1933 and recovers to almost one unconditional standard deviation above its long-term mean in 1936. Even with this most conservative measurement, the model can still account for the unemployment crisis, if one is willing to allow wages to be more inertial in the 1930s.

Our data work adds to the economic history literature. We draw heavily from the annual data on private nonfarm employment and civilian unemployment rates in [Weir \(1992\)](#), who in turn builds on the seminal work of [Lebergott \(1964\)](#). [Berridge \(1929, 1961\)](#) painstakingly collects the MetLife help-wanted index dated to 1919. [Zagorsky \(1998\)](#) compiles a historical vacancy rate series by drawing from the MetLife series. Our construction differs from Zagorsky's in many details. Finally, we draw the annual data on real output and labor productivity dated back to 1889 from [Kendrick \(1961\)](#) as well as monthly industrial production series dated back to 1884 from [Miron and Romer \(1990\)](#). We contribute to the economic history literature by performing a unified historical analysis of U.S. labor market and by applying the modern search theory to interpret the historical facts quantitatively.

Shimer (2005) shows that the unemployment volatility in the search model is too low relative to the postwar data. Hall (2005) and Hall and Milgrom (2008) show how wage rigidity increases labor market volatilities.¹ Going beyond the second moments in the postwar sample, we push the macro labor literature to explain the second and higher moments in the historical sample that includes the Great Depression. Cole and Ohanian (1999, 2004, 2007) quantify the weakness of the neoclassical growth model in explaining the weak recovery in the Great Depression. Cole and Ohanian emphasize the role of New Deal cartelization policies in explaining the weak recovery by limiting competition and increasing labor bargaining power. Also working in the neoclassical framework, Chari et al. (2007) stress the role of productivity shocks and labor market distortions in the Great Depression. We instead work with the search theory, which allows us to quantify the unemployment, vacancy, and labor market tightness dynamics in the 1930s.

Petrosky-Nadeau et al. (2018) calibrate a textbook search model with the Nash wage to output and consumption disasters in a historical cross-country panel. We differ in several crucial ways. First, we compile the historical monthly series of U.S. civilian and private nonfarm unemployment rates, vacancy rates, and labor productivity.² Second, we move beyond Nash bargaining to credible bargaining, which seems more appropriate for describing wages in the Great Depression. Finally, most important, we focus on explaining the frequency, persistence, and severity of the unemployment crises. In particular, going beyond matching moments, we feed the measured labor productivity into the model to evaluate its performance in explaining the output, unemployment, and market tightness in the 1930s.

The rest is organized as follows. Section 2 compiles the historical series and documents the long-run facts of U.S. labor market. Section 3 describes the search model of equilibrium unemployment with credible bargaining. Section 4 presents the quantitative results from matching labor market moments. Section 5 applies the model to explain the Great Depression quantitatively. Finally, Section 6 concludes.

2. U.S. labor market: historical facts

Section 2.1 compiles historical unemployment, vacancy, and labor productivity series and describes their time series properties. Section 2.2 estimates key labor market moments.

2.1. Sample construction and descriptive properties

This subsection discusses conceptual issues on our sample construction. Section A in the Online Appendix details our data sources and procedures for compiling the historical series. Our constructed historical series are available as Supplementary Data on the *Journal's* Website.

2.1.1. Unemployment rates

From January 1948 to December 2017, we use civilian unemployment rates (seasonally adjusted) from Bureau of Labor Statistics (BLS). No adjustment is necessary. Prior to 1948, we draw from Weir (1992), who provides an annual series of civilian unemployment rates from 1890 onward. We temporally disaggregate his annual series to monthly via the Denton (1971) proportional first difference procedure. The key issue is what sub-annual series to use as monthly indicators in the Denton procedure.

From January 1930 to December 1947, we use the unemployment rates from the National Bureau of Economic Research (NBER) macrohistory files (chapter 8): (i) January 1930–February 1940, series m08292a, seasonally adjusted; (ii) March 1940–December 1946, series m08292b, seasonally adjusted; and (iii) January 1947–December 1947, series m08292c, not seasonally adjusted. We pass the entire series m08292c from January 1947 to December 1966 through U.S. Census Bureau's X12 seasonal adjustment program and take the adjusted monthly observations in 1947. The Denton procedure imposes the monthly average of the interpolated series in a given year to equal that year's annual value in Weir (1992).

From January 1890 to December 1929, we use a different indicator series because the NBER series m08292a starts only in April 1929. Bai (2016) shows that the unemployment rates and the yield spread between Moody's Baa- and Aaa-rated corporate bonds have a high correlation of 0.81 from April 1929 to March 2015. Accordingly, we construct a monthly series of the yield spread: (i) NBER macrohistory series m13019 (January 1857–January 1937, American railroad bond yields, high grade); (ii) NBER macrohistory series m13019a (January 1857–December 1934, U.S. railroad bond yields); and (iii) Moody's Baa- and Aaa-rated corporate bond yields from Federal Reserve Bank of St. Louis (January 1919–December 2017). We quarterly splice the railroad yield spread (series m13019a minus series m13019) to the Moody's yield spread series (Baa minus Aaa) in the first quarter of 1919. We rescale the railroad spread series so that its monthly average in the first quarter of 1919 equals that of the Moody's series in the same quarter. We then take the values of the concatenated series from January 1890 to December 1929 as the monthly indicator.

Departing from Lebergott (1964); Weir (1992) sides with Darby (1976) in counting all government emergency workers as employed (as opposed to unemployed), a practice that is more consistent with modern definition of civilian unemployment

¹ Other explanations of the volatility puzzle include small profits (Hagedorn and Manovskii, 2008), fixed recruiting costs (Pissarides, 2009), and financial frictions (Petrosky-Nadeau and Wasmer, 2013).

² Martellini and Menzio (2018) and Petrosky-Nadeau et al. (2018) use the data in our December 2013 draft to motivate their analysis. Our data construction has since been substantially revised.

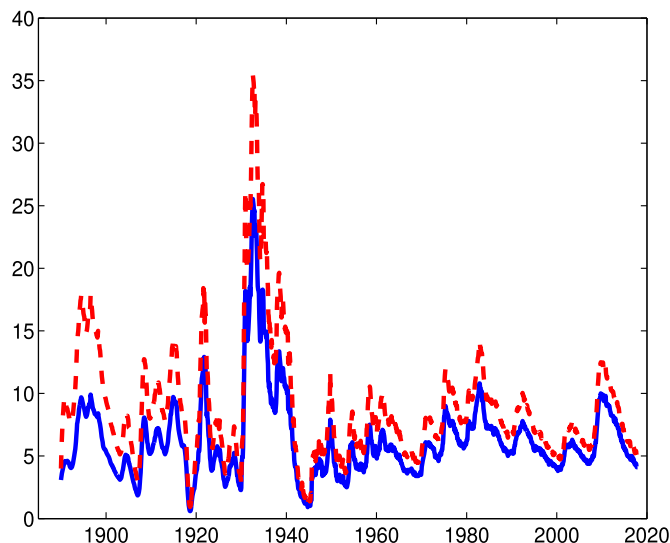


Fig. 1. U.S. monthly civilian unemployment rates and private nonfarm unemployment rates, January 1890–December 2017, 1536 months. *Note:* The blue solid line depicts civilian unemployment rates, and the red broken line private nonfarm unemployment rates. Both unemployment rates are in percent. (For interpretation of the references to color in this figure legend, the reader is referred to the web version of this article.)

rates. To address Lebergott's concern that counting these workers as unemployed more accurately depicts the failure of the private economy, Weir constructs a separate series for private nonfarm unemployment rates, by subtracting farm and government employment from both the civilian labor force and civilian employment.

Following Weir (1992), we also construct a historical series of private nonfarm unemployment rates. From January 1890 to December 1947, we use the Denton procedure to temporally disaggregate Weir's annual private nonfarm unemployment rates to monthly. The monthly indicators are the spliced yield spread series from January 1890 to December 1929 and the NBER macrohistory unemployment rates from January 1930 onward, the same indicators that we use to interpolate Weir's civilian unemployment rates. From January 1948 to December 2017, we calculate private nonfarm unemployment rates as $(\text{Civilian labor force} - \text{civilian employment}) / (\text{civilian labor force} - (\text{farm employment} + \text{government employment}))$. In the numerator, both terms should deduct the sum of farm and government employment to yield private nonfarm labor force and private nonfarm employment, respectively. As such, the numerator equals civilian unemployment, which we obtain from the Current Population Survey (CPS) released by BLS. In the denominator, we back out the sum of farm and government employment as the CPS civilian employment minus the private nonfarm employment from the Current Employment Statistics (CES) at BLS. While we acknowledge the important differences between CPS and CES (Bowler and Morisi, 2006), Weir also uses the CES-based government employment.

Fig. 1 plots the U.S. monthly civilian and private nonfarm unemployment rates from January 1890 to December 2017. The most striking feature is the extraordinarily high unemployment in the Great Depression. The mean civilian unemployment rate is 6.3% in the full sample, 6.8% in the pre-1951 sample, and 5.8% in the post-1951 sample. The median is 5.5% in the full sample, which is close to 5.6% in the post-1951 sample. However, the skewness is 2.3, and kurtosis 11.1 in the full sample, which are substantially higher than 0.6 and 3.1, respectively, in the post-1951 sample. In particular, as noted, from January 1931 to December 1939, the average is 14.8%, and the highest civilian unemployment rate reaches 25.5% in July 1932.

The contrast between the full and post-1951 samples is also stark for private nonfarm unemployment rates. The mean is 8.9% in the full sample, 10.3% in the pre-1951 sample, and 7.6% in the post-1951 sample. The median is 7.7% in the full sample, which is close to 7.3% in the post-1951 sample. However, the skewness is 2.2, and kurtosis 9.6 in the full sample, in contrast to 0.6 and 2.9 in the post-1951 sample, respectively. From January 1931 to December 1939, the average is 21.2%, and the highest unemployment rate hits 35.5% in July 1932. Such large dynamics are absent after 1951.

2.1.2. Vacancy rates

We construct a historical series for vacancy rates from January 1919 to December 2017. From December 2000 onward, we obtain the seasonally adjusted total nonfarm job openings from the Job Openings and Labor Turnover Survey (JOLTS) at BLS. This series contains government job openings. Because the series of government vacancies is not separately available prior to JOLTS, we use total nonfarm job openings throughout the sample to be consistent. From January 1995 to November 2000, we use the seasonally adjusted composite print and online help-wanted index from Barnichon and index (2010), obtained from Regies Barnichon's Web site. We quarterly splice this series to the JOLTS series in the first quarter of 2001. From January 1951 to December 1994, we use the seasonally adjusted help-wanted advertising index from the Conference Board. We quarterly splice the Conference Board series in the first quarter of 1995 to the Barnichon series (already spliced to the JOLTS series in the first quarter of 2001).

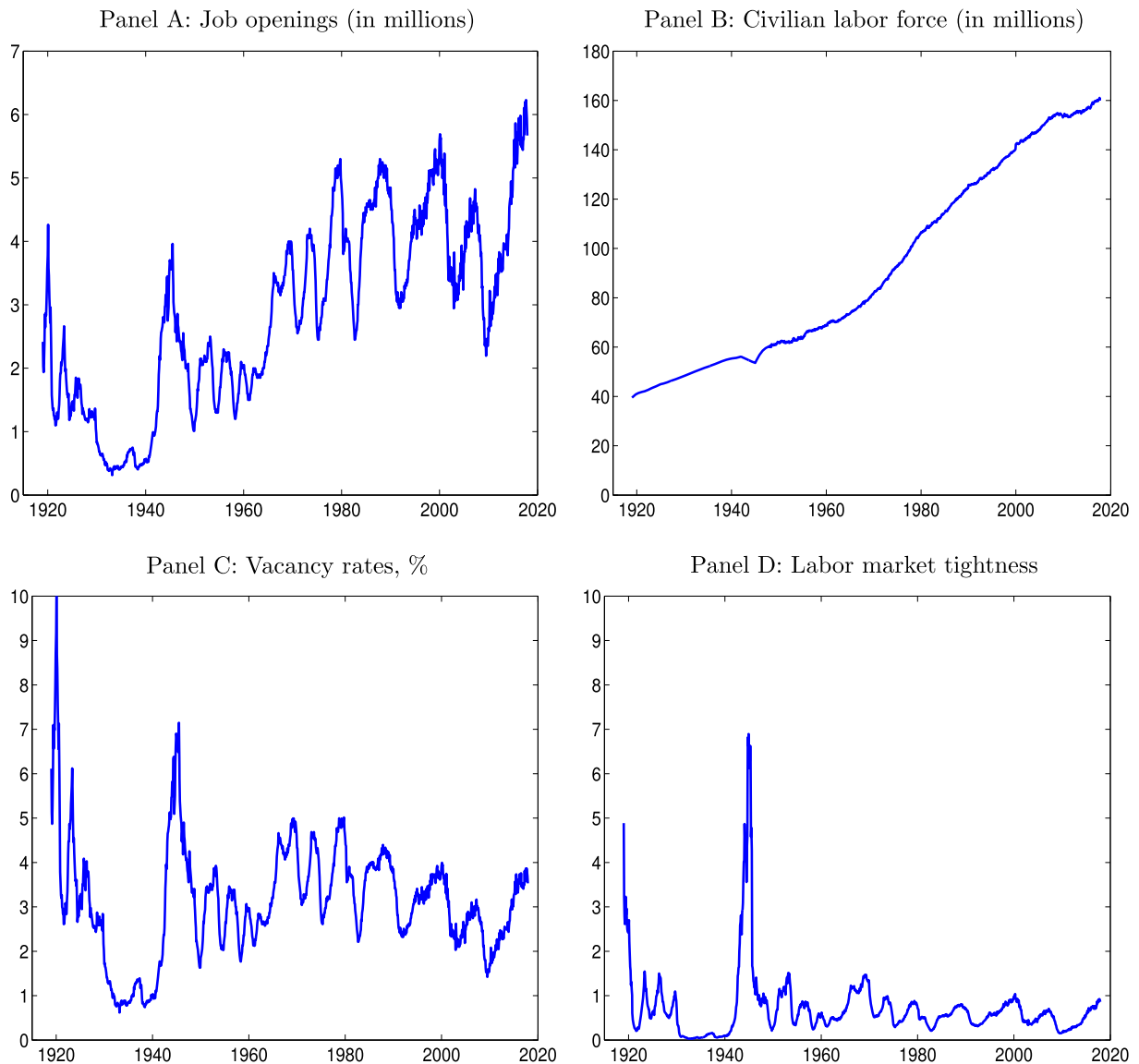


Fig. 2. U.S. monthly job openings, civilian labor force, vacancy rates, and labor market tightness, January 1919–December 2017, 1188 months. *Note:* The labor market tightness is the ratio of the vacancy rates over civilian unemployment rates.

From January 1919 to December 1950, we use the MetLife help-wanted advertising index from NBER macrohistory files (series m08082a, January 1919–August 1960, not seasonally adjusted). The Conference Board series is similar, statistically and methodologically, to the MetLife series (Preston, 1977). We seasonally adjust the MetLife series with the X12 program and quarterly splice the seasonally adjusted MetLife series in the first quarter of 1951 to the Conference Board series (already spliced to the rescaled Barnichon series).

To construct a civilian labor force series, from January 1948 to December 2017, we utilize the monthly civilian labor force over 16 years of age from the CPS (seasonally adjusted). From January 1890 to December 1947, we start with Weir (1992) annual civilian labor force series (1890–1990, 14 years and older through 1946, 16 years and older afterward). We use the Denton procedure to interpolate Weir's annual series to monthly, with a vector of ones as the monthly indicators. We then annually splice the interpolated Weir series to the CPS series in the year 1948. Finally, dividing the vacancy series by the civilian labor force series yields the historical vacancy rates from January 1919 to December 2017.

Fig. 2 plots the U.S. monthly job openings, civilian labor force, vacancy rates, and labor market tightness (vacancy rates divided by civilian unemployment rates) from January 1919 to December 2017. The average vacancy rate is 3.1% in the full sample, 2.9% prior to January 1951, and 3.2% afterward. The pre-1951 vacancy rates are clearly more volatile. The average labor market tightness is 0.7 in the full sample, 0.9 prior to 1951, and 0.6 afterward. World War II is an outlier in that the

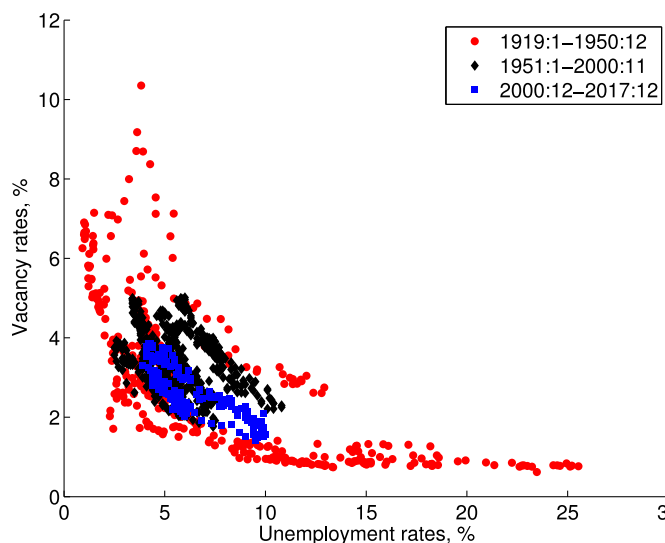


Fig. 3. The U.S. Beveridge curve, January 1919–December 2017, 1188 months. *Note:* The Beveridge curve is the scatter plot of vacancy rates versus civilian unemployment rates. (For interpretation of the references to color in this figure legend, the reader is referred to the web version of this article.)

labor market tightness reaches its highest level of 6.9 in October 1944. The aftermath of World War I might have played a role in the high tightness of 4.9 in January 1919, but sampling deficiencies might also be at work.³

Fig. 3 reports the U.S. historical Beveridge curve by plotting the vacancy rates against civilian unemployment rates from January 1919 to December 2017. Several patterns emerge. First, the scatter points display a clear convex shape, a pattern consistent with the congestion externality due to matching frictions in the labor market. Second, the pre-1951 sample shows more dramatic movements in the unemployment and vacancy rates than the post-1951 sample. When the unemployment rates exceed 20% in the Great Depression, the vacancy rates are below 1%. When the unemployment rates are below 1% during World War II, the vacancy rates hit high levels of above 6%. In contrast, such large movements are entirely absent from the post-1951 sample, in which the unemployment rates barely move above 10%, and the vacancy rates above 5%. Finally, the Great Depression, which features high unemployment rates and low vacancy rates, makes the Beveridge curve substantially flatter than it otherwise would have been. In particular, the 2007–2009 Great Recession is well aligned with the historical Beveridge curve even without the Great Depression.

2.1.3. Labor productivity

We construct a labor productivity series from January 1890 to December 2017 by dividing a series of nonfarm business real output by a series of private nonfarm employment. We obtain the following raw output data: (i) Annual private nonfarm real gross domestic product, 1889–1957, from [Kendrick \(1961\)](#); (ii) annual nonfarm business real gross value added in billions of chained 2012 dollars, 1929–2017, from National Income and Product Accounts (NIPA) Table 1.3.6., line 3, at Bureau of Economic Analysis; (iii) quarterly nonfarm business real output index, from the first quarter of 1947 to the fourth quarter of 2017, from the BLS; (iv) the Miron-Romer (1990, [Table 2](#)) monthly industrial production index, January 1884–December 1940, not seasonally adjusted; and (v) the monthly industrial production index, January 1919–December 2017, seasonally adjusted, from Federal Reserve Bank of St. Louis.

We adjust the raw output data as follows. First, we seasonally adjust the [Miron and Romer \(1990\)](#) industrial production series with the X12 program and quarterly splice the adjusted series to the Federal Reserve's industrial production series in the first quarter of 1919. Second, we annually splice Kendrick's real output series to the NIPA series in 1929. Third, from January 1889 to December 1947, we use the Denton procedure to temporally disaggregate the annual nonfarm business real output series, with the monthly industrial production series as the indicator. Fourth, from January 1947 to December 2017, we use the Denton procedure to interpolate the BLS quarterly output series, with the industrial production series as the monthly indicator. Finally, we quarterly splice the pre-1947 monthly nonfarm business real output series to the post-1947 series in the first quarter of 1947.

³ The MetLife help-wanted index is initiated in 1927 by William A. Berridge. Past issues of print newspapers are collected to gather data back to 1919, but only one-third of the newspapers in the vacancy index are obtained in 1927 ([Berridge, 1929](#)). The smaller sample might be the reason why the job openings and vacancy rates are particularly high in the early 1920s. Motivated by this concern, [Zagorsky \(1998\)](#) builds on the MetLife series only from January 1923 onward. [Berridge \(1961\)](#) also warns against "relying too heavily upon the long-run course of the full line in [Panel A of Fig. 2] or comparing the level of cycles too far apart in time. Instead, the curve's significance lies primarily in the shapes and timings of particular cycles; in those respects, the curve in its relation to employment or any other cyclical economic correlative yields useful and illuminating interpretations (p. 35, original emphasis)."

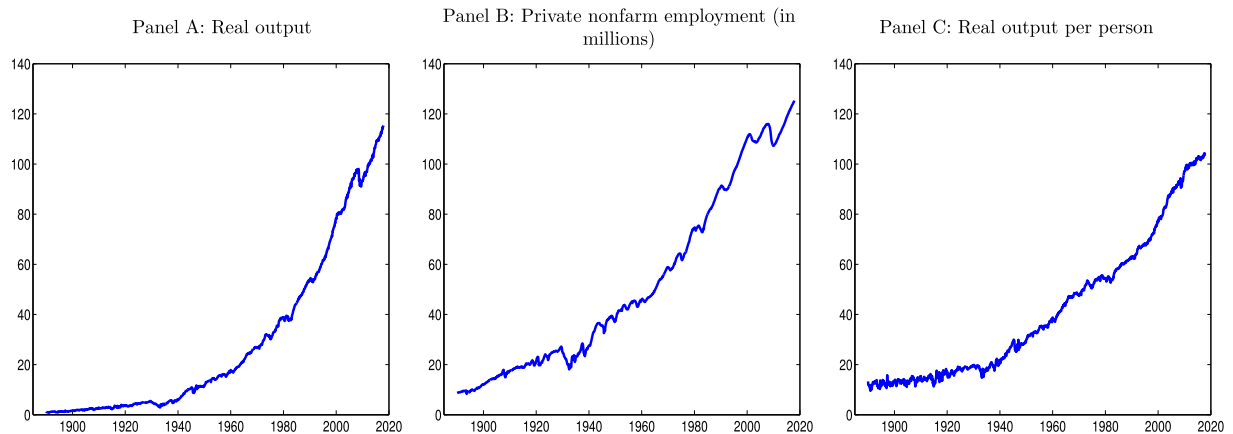


Fig. 4. U.S. monthly nonfarm business real output, private nonfarm employment, and labor productivity (real output per person), January 1890–December 2017, 1536 months. *Note:* Nonfarm business real output is an index with the value of 100 for the base year, 2012. Private nonfarm employment is number in millions. Labor productivity is an index with the value of 100 for the base year.

We also obtain: (i) Annual private nonfarm employment, number in thousands, 1890–1947, as total civilian employment minus farm employment minus government employment, all from Weir (1992, Table D3); (ii) private nonfarm employment from the CES, number in thousands, January 1939–December 2017, seasonally adjusted; (iii) index of factory employment, January 1889–December 1923, not seasonally adjusted, from NBER macrohistory series m08005; and (iv) total production worker employment in manufacturing, January 1919–March 1969, not seasonally adjusted, from NBER macrohistory series m08010b. To adjust the raw data, we first seasonally adjust NBER macrohistory series m08005 and m08010b with the X12 program and quarterly splice the adjusted m08005 to the adjusted m08010b in the first quarter of 1919. Second, we use this monthly employment series as the indicators in the Denton procedure to temporally disaggregate Weir's annual series from 1890 to 1939. Finally, we quarterly splice the interpolated monthly private nonfarm employment series to the CES monthly series in the first quarter of 1939, yielding an uninterrupted series from January 1890 to December 2017.

We then divide the monthly nonfarm business real output series by the monthly private nonfarm employment series to obtain a labor productivity series from January 1890 to December 2017. From January 1947 to December 2017, we use the Denton procedure to benchmark the monthly labor productivity series to the quarterly nonfarm business real output per job series from the BLS. Benchmarking means that we impose the average of our monthly series within a given quarter to equal the same quarter's BLS value. Finally, from January 1890 to December 1947, we quarterly splice our pre-1947 series to the benchmarked post-1947 series in the first quarter of 1947. Fig. 4 plots the series of U.S. monthly nonfarm business real output, private nonfarm employment, and labor productivity (real output per person) from January 1890 to December 2017.

2.2. Labor market moments

We report labor market volatilities and higher moments of the unemployment rates.

2.2.1. Labor market volatilities

To facilitate comparison with prior studies (Shimer, 2005), we calculate a standard set of second moments for the long sample as well as for the post-1951 sample. We take quarterly averages of monthly unemployment rates, vacancy rates, and labor productivity to convert to quarterly series, which are then detrended as log deviations from the Hodrick-Prescott (HP hereafter, 1997) trend with a smoothing parameter of 1600.

Panel A of Table 1 shows that in the historical sample, the volatility of civilian unemployment rates is 25.8%, which more than doubles the volatility of 12.6% in the post-1951 sample. The volatility of private nonfarm unemployment rates is similar to that of civilian unemployment rates, 25.7% in the 1890–2017 sample and 12.8% in the post-1951 sample (unpublished). The (civilian) unemployment-vacancy correlation is -0.79 based on their common sample from January 1919 onward but -0.92 in the postwar sample. The vacancy rate volatility is 17.2% in the 1919–2017 sample and is only somewhat higher than 13.5% in the postwar sample. The standard deviation of the labor market tightness is 37.9% in the 1919–2017 sample and is almost 50% higher than 25.6% in the post-1951 sample (Panel D, Fig. 2). More drastically, the volatility of labor productivity is 1.2% in the postwar sample, which is only about one-third of the volatility of 3.9% in the 1890–2017 sample.

If we start the sample from January 1923 onward as in Zagorsky (1998), the vacancy rate volatility is 16%, which is close to 17% in the full sample. The volatility of the labor market tightness is 36%, which is also not far from 38% in the historical sample. However, the volatility of civilian unemployment rates drops somewhat to 21%. More important, the volatility of labor productivity falls a great deal to 2.5%. The evidence suggests that the labor productivity in the early sample likely contains a fair amount of measurement errors.

Table 1
Second moments and estimated aggregate state transition probabilities of the labor market in the data, January 1890–December 2017, 1536 months.

Panel A: Second moments								
	<i>U</i>	<i>V</i>	θ	<i>X</i>	<i>U</i>	<i>V</i>	θ	<i>X</i>
	1890:1–2017:12				1951:1–2017:12			
Standard deviation	0.258	0.172	0.379	0.039	0.126	0.135	0.256	0.012
Autocorrelation	0.904	0.896	0.912	0.588	0.889	0.905	0.905	0.758
Correlation matrix	<i>U</i>	-0.791	-0.961	-0.383		-0.922	-0.979	-0.222
	<i>V</i>		0.930	0.301			0.982	0.394
	θ			0.367				0.317

Panel B: Estimated aggregate state transition probabilities, 1890:1–2017:12						
	Good Civilian unemployment rates	Bad	Crisis	Good Private nonfarm unemployment rates	Bad	Crisis
Good	95.96 (0.73)	4.04 (0.73)	0 (0)	96.09 (0.72)	3.91 (0.72)	0 (0)
Bad	4.29 (0.78)	95.16 (0.82)	0.55 (0.27)	4.86 (0.89)	94.00 (0.98)	1.13 (0.43)
Crisis	0 (0)	8.89 (11.45)	91.11 (11.45)	0 (0)	4.64 (3.18)	95.36 (3.18)
Unconditional probabilities	49.97 (6.32)	47.10 (5.94)	2.93 (2.17)	49.97 (6.87)	40.20 (5.46)	9.84 (4.85)

Note: In Panel A, the civilian unemployment rates, *U*, the vacancy rates, *V*, and the labor productivity, *X*, are converted to quarterly averages of monthly series. The labor market tightness is calculated as $\theta = V/U$. In the long sample, the *U* and *X* series are from January 1890 to December 2017, and the *V* and θ series are from January 1919 onward. The correlations involving *V* and θ are based on the sample after January 1919. Otherwise, the correlations are from the sample starting from January 1890. All the variables are in log deviations from the HP-trend with a smoothing parameter of 1600. In Panel B, the good state is identified as months in which the unemployment rates, *U*, are below the median in the sample, the bad state as months in which the *U* values are above or equal to the median but below the crisis cutoff rate of 15%, and the crisis state as months in which the *U* values are above or equal to the crisis cutoff rate. The state transition matrix is given in Eq. (1) and the transition probabilities in footnote⁵. The unconditional probabilities of the states in the last row are calculated by raising the transition matrix to the power 1000. We estimate the standard errors of the transition matrix and unconditional probabilities via bootstrapping. Specifically, we simulate 25,000 artificial samples from the estimated transition matrix. On each crisis sample (in which the maximum unemployment rate is greater than or equal to 15%), we calculate the state transition matrix and unconditional probabilities of the states. We report the cross-simulation standard deviations in parentheses. The crisis samples account for 98.2% and 99.9% of the 25,000 simulated samples of civilian and private nonfarm unemployment rates, respectively. All the probabilities and standard errors are in percent.

2.2.2. Unemployment crises

To quantify the tail behavior in the unemployment rates in Fig. 1, we follow Chatterjee and Corbae (2007) to estimate a three-state Markov chain model via maximum likelihood. The aggregate state, $\xi_t \in \{g, b, c\}$, evolves through good (*g*), bad (*b*), and crisis (*c*) states with different employment prospects. Let the transition matrix of the Markov chain be

$$P = \begin{bmatrix} p_{gg} & p_{bg} & p_{cg} \\ p_{gb} & p_{bb} & p_{cb} \\ p_{gc} & p_{bc} & p_{cc} \end{bmatrix}, \tag{1}$$

in which, for example, $p_{gb} \equiv \text{Prob}\{\xi_{t+1} = g | \xi_t = b\}$ is the probability of the economy in state *g* next period conditional on the economy in state *b* in the current period.⁴

In practice, the good state, *g*, is identified as months in which the unemployment rates are below the median. The crisis state, *c*, is months in which the unemployment rates are above or equal to 15%. The bad state, *b*, is months in which the unemployment rates are below 15% but above or equal to the median. The crisis cutoff of 15% is set such that it is relatively high, but there still exist enough months in which the economy hits the crisis state to allow us to estimate the transition probabilities (relatively) accurately.

Panel B of Table 1 reports the estimates. The crisis state is persistent in that the probability of the economy remaining in the crisis state next period conditional on it in the crisis state in the current period is 91.1% for civilian unemployment rates and 95.4% private nonfarm unemployment rates. The estimates also seem accurate, with (relatively) small bootstrapped standard errors of 11.5% and 3.2%, respectively. With probabilities of 8.9% and 4.6%, the economy switches from the crisis state to the bad state with the two unemployment rates series, respectively. Most important, unconditionally, the tail probability

⁴ As shown in Chatterjee and Corbae (2007), the maximum likelihood estimate of p_{kj} , which is the (*j*, *k*)th element of the aggregate state transition matrix, is the ratio of the number of times the economy switches from state *j* to state *k* to the number of times the economy is in state *j*. Let, for example, $\mathbf{1}_{\{\xi_t=j\}}$ denote the indicator function that takes the value of one if the economy in period *t* is in state *j* and zero otherwise. The maximum likelihood estimate of p_{kj} is given by $\hat{p}_{kj} = (\sum_{t=1}^{T-1} \mathbf{1}_{\{\xi_{t+1}=k\}} \mathbf{1}_{\{\xi_t=j\}}) / (\sum_{t=1}^{T-1} \mathbf{1}_{\{\xi_t=j\}})$.

Table 2

Second moments and the aggregate state transition matrix of the labor market in the model.

Panel A: Second moments of the labor market								
	<i>U</i>	<i>V</i>	θ	<i>X</i>	<i>U</i>	<i>V</i>	θ	<i>X</i>
	Non-crisis samples				Crisis samples			
Volatility	0.126 (0.023)	0.168 (0.017)	0.270 (0.034)	0.013 (0.001)	0.156 (0.020)	0.182 (0.013)	0.303 (0.028)	0.013 (0.001)
Persistence	0.813 (0.034)	0.615 (0.063)	0.765 (0.038)	0.771 (0.035)	0.845 (0.022)	0.600 (0.044)	0.780 (0.026)	0.782 (0.024)
Correlation	<i>U</i>	-0.681 (0.057)	-0.890 (0.019)	-0.824 (0.036)		-0.599 (0.050)	-0.876 (0.016)	-0.815 (0.027)
	<i>V</i>		0.939 (0.017)	0.939 (0.016)			0.911 (0.016)	0.913 (0.016)
	θ			0.969 (0.011)				0.971 (0.010)
Panel B: The aggregate transition matrix								
		Good	Bad	Crisis				
Good		97.93 (0.6)	2.07 (0.6)	0 (0)				
Bad		2.29 (0.66)	97.18 (0.79)	0.53 (0.38)				
Crisis		0 (0)	8.2 (10.22)	91.8 (10.24)				
Unconditional probability		49.92 (1.77)	45.31 (4.01)	4.77 (4.31)				

Note: In Panel A, we simulate 25,000 artificial samples from the model, each with 1536 months. We split the samples into two groups, non-crisis samples (in which the maximum unemployment rate is less than 15%) and crisis samples (in which the maximum rate is greater than or equal to 15%). We implement the same empirical procedure as in Panel A of Table 1 and report cross-simulation averages and standard deviations (in parentheses) conditionally on the non-crisis samples and on the crisis samples. In Panel B, on each crisis sample, we calculate the state transition matrix and unconditional probabilities of the states as in Panel B of Table 1. We report the cross-simulation averages and standard deviations in parentheses, both in percent, across the crisis samples.

of the crisis state is estimated to be 2.93% for civilian unemployment rates and 9.84% for private nonfarm unemployment rates. Their bootstrapped standard errors are 2.17% and 4.85%, respectively.

3. The model

Following Hall and Milgrom (2008), we construct a search model of equilibrium unemployment, in which the wage rate is determined via a credible bargaining game.

3.1. The setup

The model is populated by a representative household and a representative firm. The firm uses labor as the single productive input. As in Merz (1995), the household features perfect consumption insurance. The household has a continuum (with a unit mass) of members, who are, at any point in time, either employed or unemployed. The fractions of employed and unemployed workers are representative of the population at large. The household pools the income of all the members together before choosing per capita consumption. The household is risk neutral with a time discount factor of β .

The firm posts job vacancies, V_t , to attract unemployed workers, U_t . Vacancies are filled via the Den Haan et al. (2000) matching function, $G(U_t, V_t) = U_t V_t / (U_t + V_t)^{1/\iota}$, in which $\iota > 0$. Define $\theta_t \equiv V_t / U_t$ as the vacancy-unemployment (V/U) ratio (labor market tightness). The probability for an unemployed worker to find a job per unit of time (the job finding rate) is $f(\theta_t) \equiv G(U_t, V_t) / U_t = (1 + \theta_t^{-\iota})^{-1/\iota}$. The probability for a vacancy to be filled per unit of time (the vacancy filling rate) is $q(\theta_t) \equiv G(U_t, V_t) / V_t = (1 + \theta_t)^{-1/\iota}$, with $q'(\theta_t) < 0$. An increase in the scarcity of unemployed workers relative to vacancies makes it harder to fill a vacancy. As such, θ_t is the labor market tightness from the firm's perspective.

The firm incurs costs in posting vacancies. Following (Pissarides, 2009), we model the unit cost per vacancy as $\kappa_t = \kappa_0 + \kappa_1 q(\theta_t)$, in which $\kappa_0, \kappa_1 \geq 0$ are the proportional and fixed costs, respectively. The fixed cost captures training, interviewing, and administrative setup costs of adding a worker to the payroll paid after a hired worker arrives but before wage bargaining takes place. The marginal cost of hiring from the proportional cost, $\kappa_0 / q(\theta_t)$, is time-varying, but the marginal cost from the fixed cost, κ_1 , is constant. Jobs are destroyed at a constant rate of $s > 0$ per period. Employment, N_t , evolves as $N_{t+1} = (1 - s)N_t + q(\theta_t)V_t$, in which $q(\theta_t)V_t$ is the number of new hires. The size of the population is one, $U_t = 1 - N_t$. As such, N_t and U_t are also the rates of employment and unemployment, respectively. The firm takes the labor productivity, X_t , as

given. The law of motion for $x_t \equiv \log(X_t)$ is $x_{t+1} = \rho x_t + \sigma \epsilon_{t+1}$, in which $\rho \in (0, 1)$ is the persistence, $\sigma > 0$ is the conditional volatility, and ϵ_{t+1} is an independently and identically distributed standard normal shock. The firm uses labor to produce output, Y_t , with a constant returns to scale technology, $Y_t = X_t N_t$. The dividends to the firm's shareholders are given by $D_t = X_t N_t - W_t N_t - \kappa_t V_t$, in which W_t is the equilibrium wage rate.

Taking $q(\theta_t)$ and W_t as given, the firm posts an optimal number of job vacancies to maximize the cum-dividend market value of equity, subject to the employment accumulation equation and a nonnegativity constraint on vacancies, $V_t \geq 0$. Because $q(\theta_t) > 0$, this constraint is equivalent to $q(\theta_t)V_t \geq 0$. As such, the only source of job destruction in the model is the exogenous separation of employed workers from the firm.⁵ Let λ_t denote the multiplier on the nonnegativity constraint $q(\theta_t)V_t \geq 0$. The intertemporal job creation condition is given by:

$$\frac{\kappa_t}{q(\theta_t)} - \lambda_t = E_t \left[\beta \left(X_{t+1} - W_{t+1} + (1-s) \left(\frac{\kappa_{t+1}}{q(\theta_{t+1})} - \lambda_{t+1} \right) \right) \right]. \tag{2}$$

Intuitively, the marginal cost of hiring at time t equals the marginal value of employment to the firm, which in turn equals the marginal benefit of hiring at period $t + 1$, discounted to t . The marginal benefit at $t + 1$ includes the marginal product of labor, X_{t+1} , net of the wage rate, W_{t+1} , plus the next period marginal value of employment, which equals the marginal cost of hiring at $t + 1$, net of separation. The optimal vacancy policy also satisfies the Kuhn-Tucker conditions, which are given by $q(\theta_t)V_t \geq 0$, $\lambda_t \geq 0$, and $\lambda_t q(\theta_t)V_t = 0$.

3.2. Credible bargaining

To close the model, we need to specify how the equilibrium wage rate, W_t , is determined. In the most common approach, W_t is derived from the sharing rule per the outcome of a generalized Nash bargaining game between the employed workers and the firm. Let $\eta \in (0, 1)$ be the workers' relative bargaining weight and b the workers' flow value of unemployment activities. The Nash wage rate is given by $W_t = \eta(X_t + \kappa_t \theta_t) + (1 - \eta)b$. Although analytically simple, the baseline model with the Nash wage requires a very high replacement ratio (the flow value of unemployment activities over the average marginal product of labor) to yield realistically high labor market volatilities (Hagedorn and Manovskii, 2008).

3.2.1. The environment

Building on Binmore et al. (1986); Hall and Milgrom (2008) place a crucial distinction between a threat point and an outside option in the bargaining game. Bargaining takes time. Both parties make alternating offers which can be accepted, rejected to make counteroffers, or rejected to abandon the bargaining altogether. In the Nash bargaining, disagreement leads to the abandonment of the bargaining. The relevant threat point is the outside options for both parties. In contrast, in the more realistic alternating offers bargaining, disagreement only leads to another round of counteroffers. The threat point is the payoff from another round of offers, and outside options are taken only when abandoning the bargaining altogether.

The outside option for a worker is the flow value of unemployment. The outside option for the firm is to resume searching in the labor market, and its value is zero in equilibrium. During a period in which both parties engage in another round of alternating offers, the worker receives the flow value of unemployment, b , and the firm incurs the cost of delaying, $\chi > 0$. During this period, the negotiation can break down with a probability of δ . The indifference condition for a worker when considering a wage offer, W_t , is:

$$J_{N_t}^W = \delta J_{U_t} + (1 - \delta) (b + E_t [\beta J_{N_{t+1}}^{W'}]). \tag{3}$$

$J_t \equiv J(N_t, X_t)$ is the indirect utility function of the representative household. $J_{N_t}^W$ is the marginal value of an employed worker to the household when accepting the wage offer from the employer, J_{U_t} is the marginal value of an unemployed worker to the household, and $J_{N_{t+1}}^{W'}$ is the marginal value of an employed worker to the household when rejecting the firm's offer, W_t , to make a counteroffer of W'_{t+1} in the next period.

Eq. (3) says that the payoff to the worker when accepting the firm's wage offer, $J_{N_t}^W$, just equals the payoff from rejecting the offer. After rejecting the offer, with a probability of δ , the negotiation breaks down, and the worker returns to the labor market, leaving the household with the marginal value of an unemployed worker. With the probability of $1 - \delta$, the worker receives the flow value of unemployment, b , for the current period, and makes a counteroffer of W'_{t+1} to the firm in the next period, with $J_{N_{t+1}}^{W'}$ as the payoff.

The indifference condition for the firm when facing the worker's counteroffer, W'_t , is:

$$S_{N_t}^{W'} = \delta \times 0 + (1 - \delta) (-\chi + E_t [\beta S_{N_{t+1}}^W]), \tag{4}$$

in which $S_{N_t}^{W'}$ is the marginal value of an employed worker to the firm when accepting the worker's counteroffer, and $S_{N_{t+1}}^W$ is the marginal value of an employed worker when rejecting the worker's offer to make a counteroffer of W_{t+1} in the next period. Intuitively, the firm is indifferent between accepting the worker's offer W'_t and rejecting the offer to make a counteroffer of W_{t+1} next period. When rejecting the offer, the firm pays the delaying cost of χ if bargaining does not

⁵ $V_t \geq 0$ does not bind in the model's simulations under the benchmark calibration. However, because the constraint can be occasionally binding under alternative parameterizations in comparative statics, we opt to impose the constraint in the solution algorithm for computational accuracy.

break down. When it does break down, the firm's payoff is zero. Eqs. (3) and (4) collapse to the Nash conditions when the probability of breakdown, δ , equals one. During the bargaining, it is optimal for each party to make a just acceptable offer. Following (Hall and Milgrom, 2008), we assume that the firm makes the first offer, which the worker accepts. As such, W_t is the equilibrium wage, and the delaying cost is never paid.

3.2.2. The equilibrium wage

The equilibrium wage, W_t , and the worker's counteroffer wage, W'_{t+1} , can be further characterized. The marginal value of an unemployed worker to the household is:

$$J_{U_t} = b + \beta E_t [f(\theta_t) J_{N_{t+1}}^W + (1 - f(\theta_t)) J_{U_{t+1}}]. \quad (5)$$

Intuitively, the value of unemployment equals the flow value of unemployment, b , plus the discounted expected value in the next period. With a probability of $f(\theta_t)$, the unemployed worker lands a job, which delivers the value of $J_{N_{t+1}}^W$. Otherwise, the worker remains unemployed with a value of $J_{U_{t+1}}$. The marginal value of an employed worker to the household is:

$$J_{N_t}^W = W_t + \beta E_t [(1 - s) J_{N_{t+1}}^W + s J_{U_{t+1}}]. \quad (6)$$

Intuitively, the value of employment equals the flow value from the wage, W_t , plus the discounted expected value in the next period. With a probability of s , the employed worker separates from the firm and returns to the labor market as an unemployed worker with a value of $J_{U_{t+1}}$. Otherwise, the worker remains on the job, which delivers the value of $J_{N_{t+1}}^W$.

The wage offer issued by the firm to the worker, W_t , can be characterized as:

$$W_t = b + (1 - \delta) \beta E_t [J_{N_{t+1}}^W - J_{U_{t+1}}] - (1 - s - \delta f(\theta_t)) \beta E_t [J_{N_{t+1}}^W - J_{U_{t+1}}]. \quad (7)$$

From the first term in the right-hand side, W_t increases in the flow value of unemployment, b . From the second term, if the bargaining does not breakdown, W_t also increases in the surplus that the worker would enjoy after making a counteroffer, W'_{t+1} , to the firm. From the last term, W_t also increases in the separation rate, s . As s goes up, the expected duration of the job shortens. As such, the worker requires a higher wage to remain indifferent between accepting and rejecting the wage offer. Finally, W_t increases in the job finding rate. As $f(\theta_t)$ rises, the worker's outside job market prospects improve, and the firm must offer a higher wage to make the worker indifferent. However, this impact of labor market conditions on W_t becomes negligible if the probability of breakdown, δ , goes to zero.

3.2.3. Institutional background

We view the credible bargaining game as a more appropriate modeling device than the Nash bargaining game for determining the equilibrium wage during the Great Depression.

Building on Weinstein (1980), Cole and Ohanian (2004) show that 1933 New Deal cartelization policies, which are designed to limit competition and increase labor bargaining power, increase wages and prices significantly and contribute greatly to the persistence of the Great Depression. In particular, real wages and relative prices in sectors covered by the cartelization policies rise after the National Industrial Recovery Act, and subsequently the National Labor Relations Act, are adopted, and remain high. In contrast, wages and prices in sectors not covered by these policies do not rise during this period. Ohanian (2009) shows that prior to the New Deal, President Hoover's industrial labor program, along with the growing power of unions, contribute to real wage rigidity in the early stage of the Great Depression. In November 1929, Hoover met with the leaders of the major industrial firms, and requested them to not cut wages, to preferably even raise wages, and to spread work among employers. In return, labor union would not strike. By late 1931, real manufacturing average hourly earnings had raised more than 10%, and hours worked had declined more than 40%. In all, under Hoover's industrial labor program and Roosevelt's New Deal, the bargaining between firms and workers kept the wages insulated from the deteriorating labor market conditions in the 1930s.⁶

3.3. Competitive equilibrium

In equilibrium, the household receives the firm's dividends, and the goods market clears:

$$C_t + \kappa_t V_t = X_t N_t. \quad (8)$$

The competitive equilibrium consists of vacancy posting, $V_t \geq 0$, multiplier, $\lambda_t \geq 0$, consumption, C_t , and wages, W_t and W'_t , such that: (i) V_t and λ_t satisfy the intertemporal job creation condition in Eq. (2) and the Kuhn-Tucker conditions; (ii) W_t and W'_t satisfy the indifference conditions (3) and (4); and (iii) the goods market clears per Eq. (8).

4. Matching moments

Section 4.1 calibrates the model and examines its implications on labor market volatilities. Section 4.2 uses the model to explain the higher moments of unemployment.

⁶ Rose (2010) shows that Hoover's conferences delayed the cuts in hourly wages in a small number of large firms. However, the evidence might be due to characteristics of industries that the firms represent (not robust to the controls for industry characteristics).

4.1. Calibration and labor market volatilities

To solve for the model's competitive equilibrium, we adapt the globally nonlinear projection algorithm of [Petrosky-Nadeau and Zhang \(2017\)](#). The Online Appendix details the computation. Because of the strong nonlinearity in the model, steady state relations hold poorly in simulations. As such, we do not use these relations in the calibration but instead use the model's simulations from its nonlinear solution.

4.1.1. Calibration

Our calibration strategy is to match the mean and volatility of postwar civilian unemployment rates. This practice is conservative in that the postwar data have in general higher quality than the historical data. The postwar data are also widely used and well understood in the existing literature. Calibrating to the high labor productivity volatility in the prewar sample would only strengthen the crisis dynamics in the model.

As in [Gertler and Trigari \(2009\)](#), the time discount factor, β , is $0.99^{1/3}$ and the persistence of the log labor productivity, ρ , $0.95^{1/3}$. Its conditional volatility, σ , is set to be 0.00635 to match the volatility of 0.012 for the labor productivity in the postwar data ([Table 1](#)). The separation rate, s , is 3.5%, which is the average total nonfarm separation rate from December 2000 to December 2017 in JOLTS. The elasticity parameter in the matching function, ι , is 1.25, which is close to that in [Den Haan et al. \(2000\)](#). The flow value of unemployment is 0.71 ([Hall and Milgrom, 2008](#)). The probability of breakdown in bargaining, δ , is 0.1, which is close to the value of 0.0055 in their daily calibration (with 20 working days per month). The delaying cost parameter, χ , is 0.25, which is close to their value of 0.27. To calibrate the recruiting cost parameters, κ_0 and κ_1 , we target the first and the second moments of civilian unemployment rates in the postwar sample. The average unemployment rate in this sample is 5.83%, and the unemployment volatility is 12.6% ([Table 1](#)). With $\kappa_0 = 0.2$ and $\kappa_1 = 0.35$, the model implies a mean of 5.81% and a volatility of 12.6% for the unemployment rate in normal periods.

4.1.2. Labor market volatilities

To quantify the model's implications on labor market volatilities, we simulate from its stationary distribution. We start at the initial condition of zero for the log labor productivity and simulate the economy for 6000 months to reach the stationary distribution. After the burn-in, we repeatedly simulate 25,000 artificial samples, each with 1536 months. The sample length matches that in the data from January 1890 to December 2017. Because crises do not occur in every sample, we split the 25,000 samples into two groups, non-crisis (normal periods) and crisis samples. If the highest unemployment rate in a sample is greater than or equal to 15%, we categorize it as a crisis sample (otherwise a non-crisis sample). The cutoff of 15% is consistent with our empirical treatment of the historical data (Panel B of [Table 1](#)).

Panel A of [Table 2](#) reports in normal periods the unemployment volatility is 12.6%, which matches that in the postwar data. Although not a target, the labor market tightness volatility is 27% in the model, which is close to 25.6% in the data. However, the model predicts a vacancy volatility of 16.8%, which overshoots 13.5% in the data. The unemployment-vacancy correlation is -0.68 in the model, which is lower in magnitude than -0.92 in the data.

Focusing only on normal periods is subject to a selection bias that arises from ignoring the crisis samples. In the crisis samples, the unemployment volatility rises to 15.6% but falls short of 25.8% in the 1890–2017 sample in the data. A likely reason is that we calibrate the model's volatility of the labor productivity only to the postwar sample. The volatilities of vacancy and labor market tightness increase somewhat to 18.2% and 30.3%, respectively. While the former is close to 17.2%, the latter is lower than 37.9% in the historical sample. The model also predicts that the unemployment-vacancy correlation drops in magnitude from -0.68 in the non-crisis samples to -0.6 in the crisis samples. As such, the model yields a flatter Beveridge curve in the historical sample than in the postwar sample ([Fig. 3](#)). However, the magnitude of these correlations in the model is lower than that in the data.

4.2. Explaining higher moments of unemployment

More important, can the model quantitatively explain the aggregate state transition matrix and the tail probability of the unemployment crisis in [Table 1](#)? On each crisis sample (conditional on at least one crisis), we calculate the state transition matrix and unconditional probabilities of the states via the exactly same procedure in Panel B of [Table 1](#). We report the cross-simulation averages and standard deviations across the crisis samples.

Panel B of [Table 2](#) shows that the model succeeds in explaining the unemployment crisis dynamics in the data. The probability of the economy remaining in the crisis state next period conditional on the crisis state in the current period is 91.8%, which is close to 91.1% for civilian unemployment rates in the data but somewhat lower than 95.4% for private nonfarm unemployment rates. The unconditional probability of the crisis state in the model is 4.77%, which is somewhat higher than 2.93% in the data for civilian unemployment rates but lower than 9.84% for private nonfarm unemployment rates. The cross-simulation standard deviation of the 4.77% estimate in the model is 4.31%. This level of dispersion is perhaps not surprising for a tail probability estimate. In all, the model's estimates are empirically plausible.

The skewness of the model's unemployment rates is 2.06, and the kurtosis 7.9, with cross-simulation standard deviations of 0.59 and 3.62, respectively (untabulated). The skewness is close to 2.29 for civilian unemployment rates and 2.15 for private nonfarm unemployment rates in the data, but the kurtosis is lower than 11.12 and 9.61 in the data, respectively.

Table 3

Comparative statics, aggregate state transition matrix and unconditional probabilities of the three economic states in the model.

	Good	Bad	Crisis	Good	Bad	Crisis
	$\delta = 0.15$			$\chi = 0.2$		
Good	97.98	2.02	0	98.01	1.99	0
Bad	2.08	97.7	0.22	2.02	97.8	0.17
Crisis	0	17.64	82.3	0	21.55	78.41
Unconditional probability	49.85	48.36	1.76	49.78	48.89	1.31
	$\kappa_0 = 0.15$			$\kappa_1 = 0.3$		
Good	97.93	2.07	0	97.93	2.07	0
Bad	2.24	97.29	0.47	2.24	97.27	0.49
Crisis	0	11.42	88.58	0	10.92	89.07
Unconditional probability	49.89	46.32	3.79	49.89	46.17	3.94
	$s = 0.04$			$\iota = 0.9$		
Good	97.91	2.09	0	97.94	2.06	0
Bad	2.65	96.08	1.27	2.33	97.16	0.51
Crisis	0	6.22	93.78	0	5.6	94.39
Unconditional probability	49.98	40.05	9.97	49.9	44.32	5.78

Note: This table reports six comparative statics: (i) the probability of breakdown in bargaining $\delta = 0.15$; (ii) the delaying cost $\chi = 0.2$; (iii) the proportional cost of vacancy posting $\kappa_0 = 0.15$; (iv) the fixed cost of vacancy posting $\kappa_1 = 0.3$; (v) the separation rate $s = 0.04$; and (vi) the curvature of the matching function $\iota = 0.9$. In each experiment, all other parameters remain identical to those in the benchmark calibration. We simulate 25,000 artificial samples (each with 1536 months) from the model's stationary distribution. We split the samples into two groups: non-crisis samples (in which the maximum unemployment rate is less than 15%) and crisis samples (in which the maximum rate is greater than or equal to 15%). On each crisis sample, we calculate the state transition matrix and unconditional probabilities of the states per the procedure in Panel B of Table 1 and report cross-simulation averages, all in percent.

4.2.1. Comparative statics

To shed light on the intuition behind the quantitative results, we conduct an array of comparative statics: (i) the probability of breakdown in bargaining $\delta = 0.15$; (ii) the delaying cost $\chi = 0.20$; (iii) the proportional cost of vacancy posting $\kappa_0 = 0.15$; (iv) the fixed cost of vacancy posting $\kappa_1 = 0.3$; (v) the separation rate $s = 0.04$; and (vi) the curvature parameter of the matching function $\iota = 0.9$. To facilitate comparison, in each experiment, all the other parameters remain identical to those in the benchmark calibration.

Table 3 reports the comparative statics for the crisis moments. Increasing the probability of breakdown, δ , weakens the crisis dynamics. The persistence of crisis weakens from 91.8% to 82.3%, and the unconditional crisis probability falls from 4.77% to 1.76%. Raising δ also decreases labor market volatilities (the Online Appendix). Intuitively, a higher probability of breakdown in negotiation brings credible bargaining closer to the Nash bargaining, in which $\delta = 1$, giving rise to more flexible wages. As such, a higher δ makes the equilibrium wage less insulated to labor market conditions. In bad times, as the productivity drops, the wage rate also falls, providing the firm with more incentives to creating jobs. As such, the unemployment volatility falls, and the crisis dynamics dampened.

The delaying cost is also important. Reducing χ from 0.25 to 0.2 lowers the persistence of the crisis state to 78.4%, and the unconditional crisis probability to 1.31%. Reducing χ also lowers the unemployment volatility to 6.8% in normal periods. Intuitively, lower delaying costs make the equilibrium wage more responsive to labor market conditions. As such, labor market volatilities are lowered, and the crisis dynamics dampened. The proportional and the fixed costs of vacancy posting impact the results in the same direction as the delaying cost, but to a lesser quantitative extent. Reducing κ_0 to 0.15 lowers the persistence of the crisis state slightly to 88.6% and the unconditional probability to 3.79%. Similarly, reducing κ_1 to 0.3 drops the persistence of the crisis state slightly to 89.1% and the unconditional probability to 3.94%. Intuitively, lower vacancy costs stimulate job creation flows so as to starve off unemployment crises.

A separation rate, s , of 4% makes the crises more frequent and persistent. The persistence goes up to 93.8%, and the unconditional probability to 9.97%. Intuitively, because jobs are destroyed at a higher rate, all else equal, the economy is less capable of offsetting job destruction flows through job creation. As such, the crisis dynamics are strengthened.

Reducing the curvature of the matching function, ι , to 0.9 strengthens the crisis dynamics. The persistence of the crisis state increases to 94.4%, and its unconditional probability to 5.78%. Intuitively, a decrease in ι increases the elasticity of new hires with respect to vacancies. This elasticity is given by $1/(1 + \theta_t^l)$, and a lower ι means a higher elasticity for $\theta_t^l > 1$, which holds most of the time in simulations. As vacancies fall in recessions, new hires drop faster with a lower ι , meaning that the congestion effect for unemployed workers becomes more severe. As such, the crisis dynamics are reinforced.

5. Explaining the great depression

Most important, going beyond matching moments, we feed the measured labor productivity in the data into the model, calculate the model's sample paths, and compare them with those in the Great Depression. We closely follow (Cole and Ohanian, 1999; 2007) test design in accounting for the Great Depression. To facilitate comparison with their work, we work with annual data. Real output per capita is nonfarm business real gross value added in chained dollars (NIPA Table 1.3.6, line 3) divided by working-age population (NIPA Table 7.1, line 18). The sample is from 1929 to 2017. For private nonfarm employment, from 1939 onward, we time-aggregate the CES monthly series to annual by taking the monthly average of a given year as the year's annual value. We then annually splice Weir's (1992) to the CES's annual series in the year of 1939.

We detrend the entire 1929–2017 series of real output per capita and private nonfarm employment per capita as log deviations from their respective HP trend with an annual smoothing parameter of 25. This value is higher than 6.25, which, per Ravn and Uhlig (2002), matches the popular value of 1600 for quarterly data in Hodrick and Prescott (1997).⁷ Our value of 25 corresponds to the quarterly value of 6400. Hodrick and Prescott's Table 1 shows that this value yields quantitatively similar cyclical output dynamics as 1600 in the postwar data. We use a higher value of 25 because 6.25, which is calibrated to measure shorter business cycle fluctuations in the postwar data, tends to treat the large movements in the Great Depression as changes in the trend rather than deviations from the trend (Cole and Ohanian, 2007, p. 23–24).

Labor productivity is detrended real output per capita divided by the detrended employment per capita. For comparison, we also examine an alternative labor productivity series from Kendrick (1961) (Table A-XXIII, output per person, 1889–1957). We detrend the Kendrick series as log deviations from its HP trend with the smoothing parameter of 25. Finally, the data are annual, but the model's frequency is monthly. We linearly interpolate our and Kendrick's detrended labor productivity series into monthly and feed their logarithms into the model to trace out its implied sample paths in the 1930s.

Reassuringly, as shown in Panel A of Fig. 5, although Kendrick (1961) measures real output differently from NIPA and private nonfarm employment differently from Lebergott (1964) and Weir (1992), our labor productivity series and Kendrick's are fairly close. With the 1929 level scaled to 100, our series drops to its lowest point of 89, and Kendrick's to 88.8, in 1933. Both series then recover and largely return to their trend level in 1936, with our series at 100.4 and Kendrick's 99.8. Both fall afterward, with our series standing at 92.7, and Kendrick's 94.8, in 1939. In terms of the deviation from its long-term mean, our log labor productivity hits -11.7% in 1933, which amounts to 3.4 times of its unconditional volatility of 3.46% in the postwar sample. ($\sigma/\sqrt{1-\rho^2}$, with $\sigma = 0.00635$ and $\rho = 0.983$). The log productivity remains at -7.6% in 1939, which is about 2.2 times of its unconditional volatility.

The red dashed line in Panel B of Fig. 5 shows the detrended real output per capita in the NIPA data. With the 1929 level scaled to 100, real output falls to 73.7 in 1933, recovers to 94.9 in 1936, but falls again to 81.1 in 1939. The model path (the blue solid line) based on our labor productivity does a good job in tracing the general pattern, with a steeper decline to 64.3 in 1933, a somewhat stronger recovery to 98.3 in 1936, and a lower level of 76.4 in 1939. The model path based on Kendrick's labor productivity is quantitatively close.

Most important, Panel C shows that the model does a good job in explaining the unemployment crisis in the Great Depression. In the data, civilian unemployment rates (the red dashed line) reach the highest level, 23.5%, and private nonfarm unemployment rates (the magenta dotted line), 33.4%, in March 1933. The model predicts very high unemployment rates, all of which are above 32%, from March to August 1933, but the highest, 32.9%, is in June 1933. Unemployment rates fall afterward both in the model and in the data, but the drop is steeper in the former than in the latter. The model predicts unemployment rates in the 5.6%–8.8% range in 1936, in contrast to the 9.2%–11% range for civilian unemployment rates and 13.5%–16.4% for private nonfarm unemployment rates in the data. After 1936, unemployment rates are persistently high both in the model and in the data. Panel D reveals a weakness of the model in explaining the persistence of labor market tightness. While the market tightness in the data is persistently low in the 1930s (the red dashed line), the tightness in the model spikes up to the 1929 level in 1936, although it does fall back to the same level as in the data afterward (the blue solid and black dashdot lines).⁸

5.1. The impact of detrending

To quantify the impact of the smoothing parameter in the HP filter, Fig. 6 reports the comparative statics from a wide range of values. The lowest value is 6.25 Ravn and Uhlig (2002), and the highest is infinity (linear detrending). Several interesting results emerge. First, the broad patterns based on a smoothing parameter of 25 are quantitatively similar over a large interval of smoothing parameters that range from 18.75 to 37.5. These two annual values correspond to the quarterly values of 4800 and 9600, which amount to three and six times of the popular value of 1600, respectively. Intuitively, a

⁷ Ravn and Uhlig (2002) show that the smoothing parameter should be adjusted by the fourth power of the observation frequency ratio. The quarterly-to-annual frequency ratio is four. As such, the annual parameter that matches the quarterly parameter of 1600 should be $1600/4^4 = 6.25$.

⁸ Because of the trading externality of the matching technology, the upward spike in labor market tightness does not lead to an equally large drop in the unemployment rate in Panel D of Fig. 7. Intuitively, when many vacancies compete for a small pool of unemployed workers, the entry of an additional vacancy causes a large drop in the vacancy-filling rate. This externality raises (at an increasing speed) the marginal cost of hiring, which is in turn convex in the labor productivity. Consequently, the unemployment rate falls only gradually as labor market conditions improve (Petrosky-Nadeau et al., 2018). The scatterplots in Figure A.1. in the Online Appendix illustrate this mechanism in our credible bargaining model.

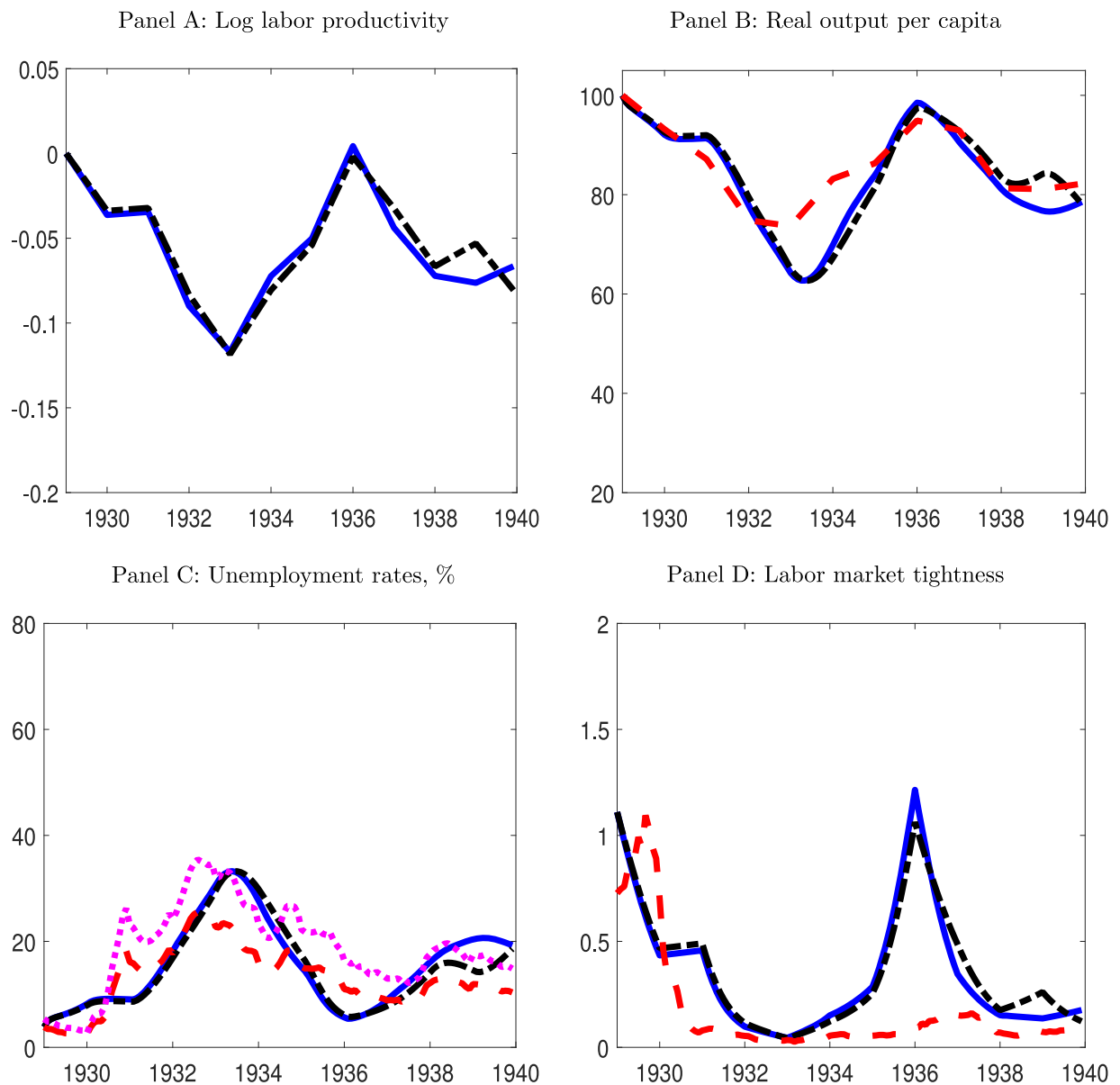


Fig. 5. Accounting for the Great Depression, January 1929–December 1939. *Note:* Annual data on nonfarm business real output and working-age population are from NIPA and private nonfarm employment from Weir (1992) and CES. Kendrick's (1961) labor productivity series is from his Table A-XXIII, 1889–1957. Real output and employment per capita and Kendrick's labor productivity are detrended as log deviations from the HP trend with a smoothing parameter of 25. Our labor productivity is real output over employment, both detrended. We linearly interpolate our and Kendrick's annual labor productivity series into monthly and feed their logarithms into the model to calculate the model's implied output, unemployment rates, and labor market tightness series. The model paths from our labor productivity series are plotted as blue solid lines, and those from Kendrick's series as black dashdot lines. Red dashed lines plot the corresponding series in the data, and the magenta dotted line in Panel C plots private nonfarm unemployment rates in the data. (For interpretation of the references to color in this figure legend, the reader is referred to the web version of this article.)

larger smoothing parameter gives rise to a more volatile cyclical component in the measured labor productivity, which in turn yields stronger unemployment crises in the model.

Second, in the extreme case of linear detrending, real output per capita falls dramatically from 100 in 1929 to 58.1 in 1933, recovers to 77.5 in 1936, and remains at 76.3 in 1939. The log labor productivity hits the lowest level of -20% in 1933, which amounts to 5.8 times of its unconditional volatility of 3.46%. The log productivity remains at -9.32% in 1939, which is about 2.7 times of its unconditional volatility. In the presence of such extreme shocks, the model overestimates the output decline and unemployment rates in the 1930s, although the market tightness is persistently low. The model's paths with a smoothing parameter of 100 are not far from those with linear detrending. In our view, shocks of more than 5.5 unconditional standard deviations are unrealistic, probably an artifact from the detrending method. In particular, Hodrick

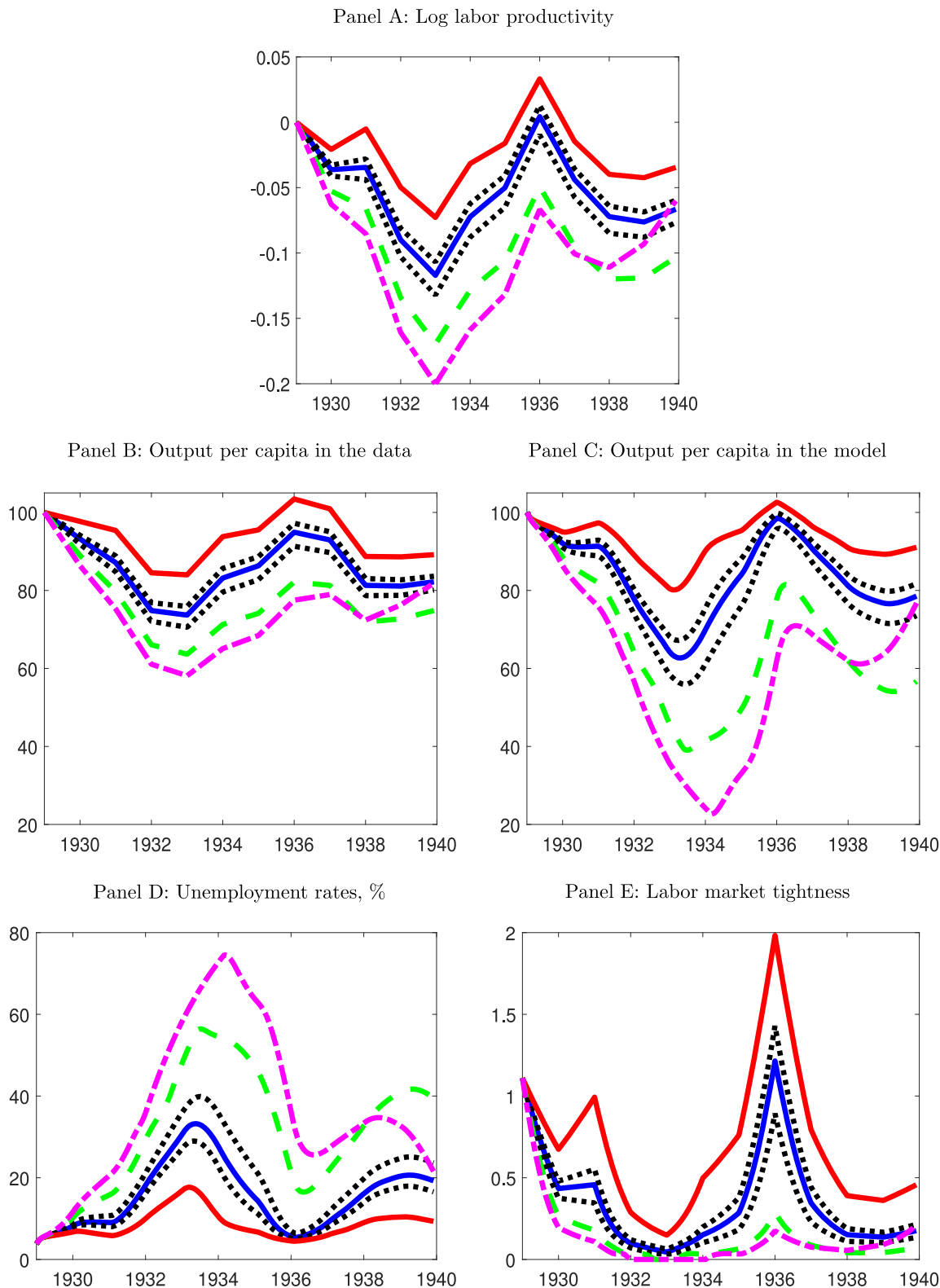


Fig. 6. Accounting for the Great Depression, the impact of detrending, January 1929–December 1939. Note: This figure shows the impact of varying the smoothing parameter in the HP filter. The blue solid lines are for the value of 25 (the benchmark case in Fig. 5). The two black dotted lines are for 18.75 and 37.5. The green dashed lines are for the value of 100, the magenta dash-dot lines for the value of infinity (linear detrending), and the red solid lines are for the value of 6.25. (For interpretation of the references to color in this figure legend, the reader is referred to the web version of this article.)

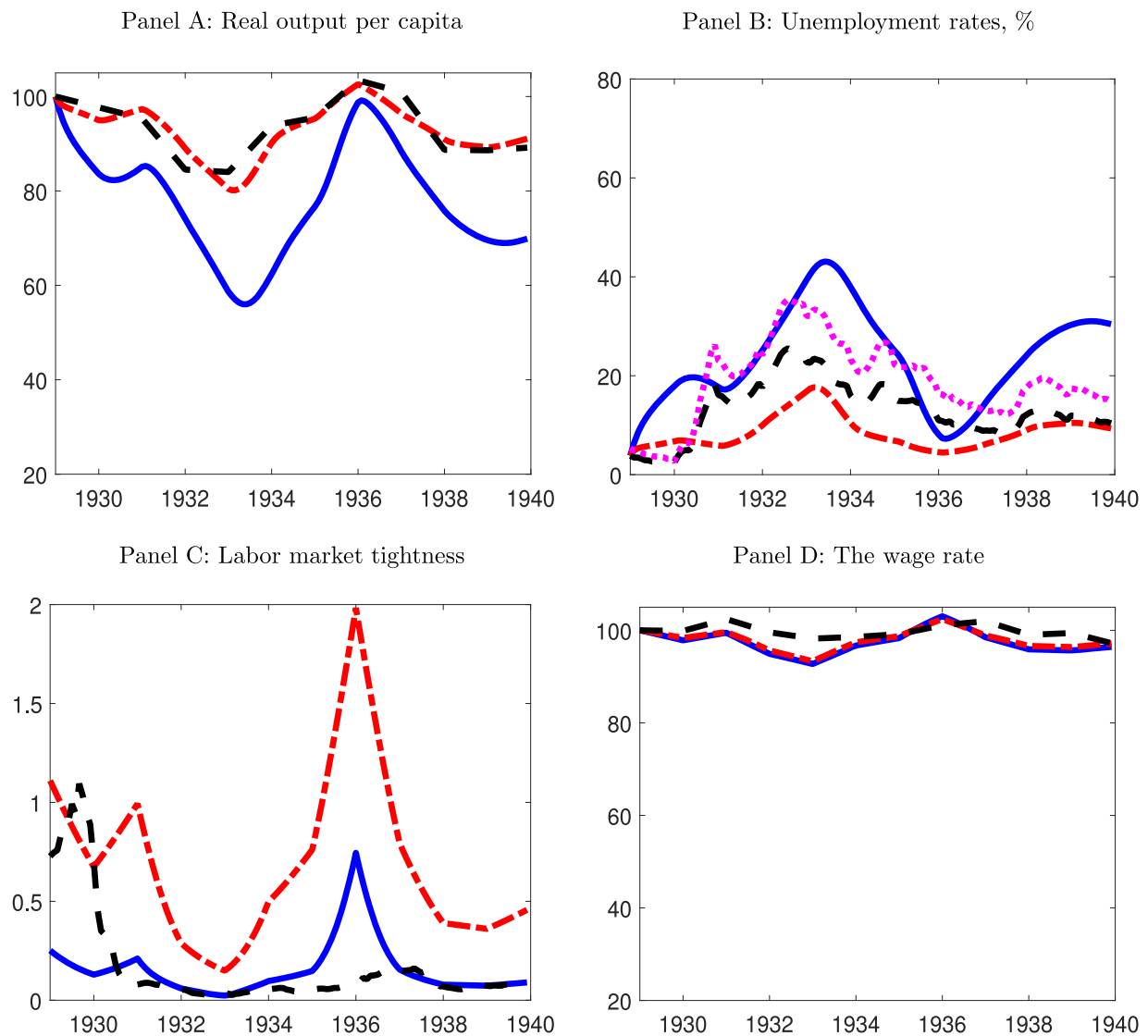


Fig. 7. Accounting for the Great Depression, the impact of credible bargaining, January 1929–December 1939. *Note:* This figure shows the impact of changing the probability of bargaining breakdown, δ , to 0.075 and the delaying cost, χ , to 0.3. The model paths with these alternative parameter values are in blue solid lines, and those with the benchmark values of $\delta = 0.1$ and $\chi = 0.25$ in red dashed lines. Black dashed lines plot the corresponding series in the data, and the magenta dotted line in Panel B depicts private nonfarm unemployment rates in the data. (For interpretation of the references to color in this figure legend, the reader is referred to the web version of this article.)

and Prescott (1997) emphasize that linear detrending violates the assumption that no unit root gives rise to nonstationarity in the cyclical component. Finally, in the other extreme case with the smoothing parameter of 6.25, real output per capita in the data falls only to 84 in 1933, recovers to the above-trend levels of 103.4 in 1936 and 100.9 in 1937, and drops back to 88.6 in 1939. The above-trend recovery in 1936 indicates that the smoothing parameter of 6.25 is too low, since it appears to treat large cyclical components as changes in the trend. With the same smoothing parameter, the log labor productivity hits the lowest level of -7.3% in 1933, which is about 2.1 times of its unconditional standard deviation. The log productivity recovers to $+3.3\%$ in 1936, which is almost one unconditional standard deviation above its long-term mean. With this labor productivity series, the model still predicts a high unemployment rate of 18.1% in March 1933. However, the predicted unemployment rates in 1936 are low, ranging only from 4.5% to 5.9%.

5.2. The impact of credible bargaining

We have shown that with a smoothing parameter of 25, which implies a large shock to the log labor productivity, the model can account for the depth and persistence of the unemployment crisis in the Great Depression. Alternatively, 25 might

still be too high. Equivalently, our measured productivity shock, which amounts to 3.4 unconditional standard deviations below the long-term mean, might still be too large. In this subsection, we show that even under the most conservative measurement with a smoothing parameter of 6.25, the model can still account for the Great Depression, if one is willing to entertain the possibility that wages are more inertial in the 1930s than in the postwar periods.

A large literature suggests that real wages might be more distorted in the 1930s. As noted, President Hoover's industrial labor program and President Roosevelt's New Deal cartelization policies collectively raised labor bargaining power and made wages less affected by adverse labor market conditions (Cole and Ohanian, 2004; Ohanian, 2009). Also, the gold standard transmits globally contractionary monetary shocks originated in the United States (Eichengreen and Sachs, 1985). Despite deflation, nominal wages adjust slowly (Bernanke and Carey, 1996; Bordo et al., 2000).

In the model, we capture the excessive wage inertia in the 1930s by adjusting the two key parameters for credible bargaining. We use a lower probability of bargaining breakdown, δ , 0.075, and a higher delaying cost, χ , 0.3, in contrast to 0.1 and 0.25 in the benchmark calibration. Both changes make equilibrium wages more insulated from labor market conditions. From Fig. 7, with the 1929 level scaled to 100, the model predicts an output decline to 58.7 in 1933 (Panel A) and the highest unemployment rate of 43.1% in June 1933 (Panel B). Output recovers close to the trend in 1936, and the unemployment rate falls to 7.2% in March of the same year. The economy deteriorates afterward, with output falling back to around 70 and the unemployment rate rising to around 30% in 1939. The upward spike in labor market tightness in 1936 with the low- δ -high- χ calibration is less than one half of that with the benchmark calibration (Panel C). Finally, the wage rate is inertial (Panel D), especially when compared with the large drops in output in Panel A. However, the wage rate in the model is somewhat less rigid than the wage rate in the data (Section A.4 in the Online Appendix details the measurement). A likely reason is that deflation in the 1930s is left outside the model.⁹

6. Conclusion

Empirically, drawing from a variety of rarely used data sources, we compile historical monthly series of U.S. unemployment rates, vacancy rates, and labor productivity, some of which date back to January 1890. Theoretically, a search model of equilibrium unemployment with credible bargaining, despite being calibrated to the mean and volatility of postwar unemployment rates, potentially explains the unemployment crisis in the Great Depression. The frequency, persistence, and severity of the unemployment crises in the model are all quantitatively consistent with those in the historical data. All in all, intriguingly, a unified search model of equilibrium unemployment with the same parameters is a good start to explaining labor market dynamics in both the prewar and postwar samples simultaneously.

Supplementary material

Supplementary material associated with this article can be found, in the online version, at doi:[10.1016/j.jmoneco.2020.01.009](https://doi.org/10.1016/j.jmoneco.2020.01.009)

CRedit authorship contribution statement

Nicolas Petrosky-Nadeau: Conceptualization, Methodology, Software, Formal analysis, Investigation, Data curation, Writing - review & editing. **Lu Zhang:** Conceptualization, Methodology, Software, Validation, Formal analysis, Investigation, Data curation, Writing - original draft, Writing - review & editing, Visualization, Supervision, Project administration.

References

- Bai, H., 2016. Unemployment and Credit Risk. Working Paper. University of Connecticut.
- Barnichon, R., 2010. Building a composite help-wanted index. *Econ. Lett.* 109, 175–178.
- Bernanke, B.S., Carey, K., 1996. Nominal wage stickiness and aggregate supply in the great depression. *Q. J. Econ.* 111, 853–883.
- Berridge, W.A., 1929. Labor turnover. *Month. Labor Rev.* 29, 62–65.
- Berridge, W.A., 1961. Observations on metropolitan life's help-wanted advertising index — and “welcome to the conference board!”. *Conf. Board Bus. Rec.* 32–37.
- Binmore, K., Rubinstein, A., Wolinsky, A., 1986. The nash bargaining solution in economic modelling. *Rand J. Econ.* 17, 176–188.
- Bordo, M.D., Erceg, C.J., Evans, C.L., 2000. Money, sticky wages, and the great depression. *Am. Econ. Rev.* 90, 1447–1463.
- Bowler, M., Morisi, T.L., 2006. Understanding the employment measures from the CPS and CES survey. *Month. Labor Rev.* 23–38.
- Chari, V.V., Kehoe, P.J., McGrattan, E.R., 2007. Business cycle accounting. *Econometrica* 75, 781–836.
- Chatterjee, S., Corbae, D., 2007. On the aggregate welfare cost of great depression unemployment. *J. Monet Econ* 54, 1529–1544.
- Cole, H.L., Ohanian, L.E., 1999. The great depression in the United States from a neoclassical perspective. *Q. Rev.* 2–24. Winter
- Cole, H.L., Ohanian, L.E., 2004. New deal policies and the persistence of the great depression: a general equilibrium analysis. *J. Political Econ.* 112, 779–812.
- Cole, H.L., Ohanian, L.E., 2007. A Second Look at the U.S. Great Depression from a Neoclassical Perspective. In: Kehoe, T.J., Prescott, E.C. (Eds.), *Great Depressions of the Twentieth Century*. Federal Reserve Bank of Minneapolis, Minneapolis.
- Darby, M.R., 1976. Three-and-a-half million u.s. employees have been mislaid: or, an explanation of unemployment, 1934–1941. *J. Political Econ.* 84, 1–26.

⁹ From Panel D of Fig. 7, the wage rate with the low- δ -high- χ calibration is fairly close to the wage rate with the benchmark calibration. Plotting the two wage rates against the log labor productivity based on the model's optimal solution, Figure A.2. in the Online Appendix verifies that the former is indeed more inertial than the latter, especially when the log productivity is very low. Overall, the results indicate the power of the wage inertia mechanism in the model. In particular, a seemingly small difference in the wage dynamics can give rise to large differences in the output and unemployment dynamics.

- Den Haan, W.J., Ramey, G., Watson, J., 2000. Job destruction and propagation of shocks. *Am. Econ. Rev.* 90, 482–498.
- Denton, F.T., 1971. Adjustment of monthly or quarterly series to annual totals: an approach based on quadratic minimization. *J Am Stat Assoc* 66, 99–102.
- Eichengreen, B., Sachs, J., 1985. Exchange rates and economic recovery in the 1930s. *J. Econ. Hist.* 45, 925–946.
- Gertler, M., Trigari, A., 2009. Unemployment fluctuations with staggered nash wage bargaining. *J. Political Econ.* 117, 38–86.
- Hagedorn, M., Manovskii, I., 2008. The cyclical behavior of equilibrium unemployment and vacancies revisited. *Am. Econ. Rev.* 98, 1692–1706.
- Hall, R.E., 2005. Employment fluctuations with equilibrium wage stickiness. *Am. Econ. Rev.* 95, 50–65.
- Hall, R.E., Milgrom, P.R., 2008. The limited influence of unemployment on the wage bargain. *Am. Econ. Rev.* 98, 1653–1674.
- Hodrick, R.J., Prescott, E.C., 1997. Postwar U.S. business cycles: an empirical investigation. *J Money Credit Bank* 29, 1–16.
- Kendrick, J.W., 1961. *Productivity Trends in the United States*. Princeton University Press, Princeton.
- Lebergott, S., 1964. *Manpower in economic growth: The american record since 1800*. McGraw-Hill Inc., New York.
- Martellini, P., Menzio, G., 2018. Declining Search Frictions, Unemployment and Growth. Working Paper. National Bureau of Economic Research.
- Merz, M., 1995. Search in labor market and the real business cycle. *J Monet Econ* 95, 269–300.
- Miron, J.A., Romer, C.D., 1990. A new monthly index of industrial production. *J. Econ. Hist.* 50, 321–337.
- Ohanian, L.E., 2009. What—or who—started the great depression. *J Econ Theory* 144, 2310–2335.
- Petrosky-Nadeau, N., Wasmer, E., 2013. The cyclical volatility of labor markets under frictional financial market. *Am. Econ. J.* 5, 193–221.
- Petrosky-Nadeau, N., Zhang, L., 2017. Solving the diamond-mortensen-pissarides model accurately. *Quant Econom* 8, 611–650.
- Petrosky-Nadeau, N., Zhang, L., Kuehn, L., 2018. Endogenous disasters. *Am. Econ. Rev.* 108, 2212–2245.
- Pissarides, C.A., 2009. The unemployment volatility puzzle: is wage stickiness the answer? *Econometrica* 77, 1339–1369.
- Preston, N.L., 1977. *The Help-wanted Index: Technical Description and Behavioral Trends*. The Conference Board, New York.
- Ravn, M.O., Uhlig, H., 2002. On adjusting the hodrick-prescott filter for the frequency of observations. *Rev. Econ. Stat.* 84, 371–380.
- Rose, J.D., 2010. Hoover'S truce: wage rigidity in the onset of the great depression. *J. Econ. Hist.* 70, 843–870.
- Shimer, R., 2005. The cyclical behavior of equilibrium unemployment and vacancies. *Am. Econ. Rev.* 95, 25–49.
- Weinstein, M.M., 1980. *Recovery and Redistribution under the NIRA*. North-Holland Publishing Company, Amsterdam.
- Weir, D.R., 1992. A century of u.s. unemployment, 1890–1990: revised estimates and evidence for stabilization. *Res Econ Hist* 14, 301–346.
- Zagorsky, J.L., 1998. Job vacancies in the United States: 1923 to 1994. *Rev/ Econ. Stat.* 80, 338–345.